PERGAMON

International Journal of Solids and Structures 38 (2001) 3263–3280

INTERNATIONAL JOURNAL OF SOLIDS and STRUCTURES

www.elsevier.com/locate/ijsolstr

Numerical models for nonlinear analysis of elastic shells with eigenmode-affine imperfections

J.G. Teng *, C.Y. Song

Department of Civil and Structural Engineering, The Hong Kong Polytechnic University, Hung Hom, Kowloon, Hong Kong

Received 10 December 1999; in revised form 13 May 2000

Abstract

Nonlinear finite-element analysis provides a powerful tool for assessing the buckling strength of shells. Since shells are generally sensitive to initial geometric imperfections, a reliable prediction of their buckling strength is possible only if the effect of geometric imperfections is accurately accounted for. A commonly adopted approach is to assume that the imperfection is in the form of the bifurcation buckling mode (eigenmode-affine imperfection) of a suitable magnitude. For shells of revolution under axisymmetric loads, this approach leads to the analysis of a shell with periodically symmetric imperfections. Consequently, sector models spanning over one or half the circumferential wave of the imperfection may be considered adequate. This paper presents a study which shows that a simple nonlinear analysis of the imperfect shell may not deliver the correct buckling load, due to the tendency of the shell to develop mode changes in the deformation process before reaching the limit point. This inadequacy exists not only with short sector models (half-wave or whole-wave models) but also with more complete models (half-structure or whole-structure models) for different reasons. The paper concludes with recommendations on the proper use of the four different kinds of models mentioned above in determining shell buckling strengths.

Keywords: Numerical models; Shells; Elastic; Imperfections; Nonlinear analysis; Buckling; Bifurcation; Post-buckling

1. Introduction

Existing shell buckling research has been largely concentrated on shells of simple geometries subject to simple loading conditions, with only limited information on more complex problems (Teng, 1996). This limitation of existing research is passed on to design codes for thin shell structures, which generally provide stability design rules only for simple cases. Many shell structures, particularly civil engineering metal shell structures, may possess a complex structural form and have to be designed to avoid buckling failure under complex load combinations (e.g. gravitational loads + wind loads). For such complex situations, simple design rules are not available in design codes, so nonlinear finite element analysis has been suggested for direct use in design for assessing the buckling strength of shells (Teng, 1996). Some example shell buckling

* Corresponding author. Current address: Department of Civil and Structural Engineering, The Hong Kong Polytechnic University, Hong Kong, China. Tel.: +852-2766-6012; fax: +852-2334-6389.

E-mail address: cejgteng@polyu.edu.hk (J.G. Teng).

0020-7683/01/$ - see front matter
PII: S0020-7683(00)00222-5

problems for which simple design rules do not exist can be found in Teng (1996) and Rotter (1998). Rotter (1998) also outlines the background to the development of the European code for steel shell structures where codified guidance for the direct application of numerical nonlinear and buckling analysis is provided for the first time.

Since shells are generally sensitive to initial geometric imperfections, a reliable prediction of their buckling strength is possible only if the effect of geometric imperfections is accurately accounted for, in addition to the proper modelling of geometric and material nonlinearities for which suitable techniques exist, at least for metal shells.

Imperfections in shells are not known at the design stage, so in order to assess the buckling strength of a shell at the design stage, both the form and amplitude of the expected imperfection have to be specified based on certain assumptions or prior knowledge. While statistically-based geometric imperfection models (Chryssanthopoulos, 1991a,b; Arbocz, 1997) for a given processes of fabrication are the most rational, they rely on a large number of surveys on full-scale structures and are not yet available for many shell structures such as most steel shell structures in civil engineering applications. The most commonly adopted approach in the numerical assessment of shell buckling strength is thus to assume a certain unfavourable form of geometric imperfection with the amplitude linked to fabrication tolerance. Such imperfections are referred to as equivalent imperfections as they are intended to cause as much strength reduction as may be expected of actual imperfections in real shells. Limited studies (Schmidt and Krysik, 1991; Speicher and Saal, 1991) have been carried out on the specification of simple equivalent geometric imperfections.

A commonly adopted approach for specifying geometric imperfections is to assume that the imperfection is in the form of the bifurcation buckling mode (eigenmode-affine imperfection) of a suitable magnitude. This approach has been recommended by the newly developed European code for steel shell structures (ENV 1993-1-6, 1999) unless a different unfavourable pattern can be justified. At first thought, the determination of the buckling load of a shell seems straightforward once the imperfection form and amplitude are given. This simple view, however, is often over optimistic.

This paper presents a study on the determination of buckling strengths of shells of revolution under torsionless axisymmetric loads using this eigenmode-affine imperfection approach. For such shells, this approach leads to the analysis of a shell with periodically symmetric imperfections around the circumference. Consequently, sector models spanning over one or half the circumferential wave of the imperfection may be considered adequate. This study shows that a simple nonlinear analysis of the imperfect shell may not deliver the correct buckling load, due to the tendency of the shell to develop a mode change in the deformation process before reaching the limit point. This inadequacy exists not only with short sector models (half-wave or whole-wave models) but also with more complete models (half-structure or whole-structure models) for different reasons. The paper concludes with recommendations on the proper use of the four different kinds of models mentioned above in determining shell buckling strengths.

All numerical results presented in this paper were obtained using the nine-node doubly curved thin shell element available in the general-purpose computer program ABAQUS (Hibbit, Karlsson & Sorensen, 1998) which has been widely used by the shell buckling research community. A different set of issues exists if an axisymmetric shell element is used, a discussion of which is beyond the scope of the present paper. Most of the points are illustrated using a cylinder subject to a radial ring load at mid-height (Fig. 1), while the externally pressurized cylinder is used in the final part of the paper.

2. Numerical models

A perfect axisymmetrically loaded shell of revolution may bifurcate into a nonsymmetric buckling mode consisting of periodic waves around the circumference unless axisymmetric buckling precedes nonsymmetric bifurcation. This paper is concerned only with shells of revolution which buckle into a nonsymmetric

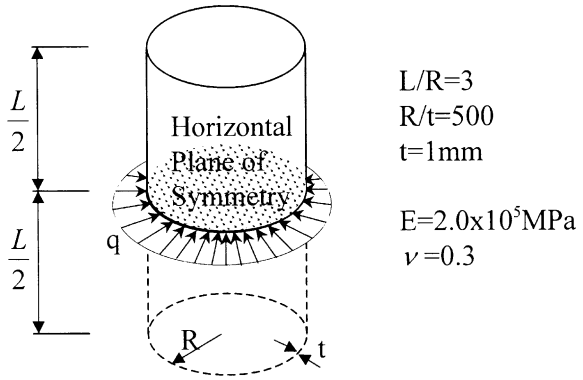

Fig. 1. Cylinder under a radial ring load at mid-height.

periodic mode. Since the buckling mode exhibits periodical symmetry, for nonlinear analysis of a shell of revolution with an eigenmode-affine imperfection using a general shell element, a number of different numerical models may be used as listed in Table 1. The meridional edges of the sector models and the half-structure model are given symmetric boundary conditions, in accordance with the expected periodical symmetry of deformations in such a shell.

A shell of revolution with a significant eigenmode-affine imperfection is expected to deform in the mode imposed by the imperfection during a nonlinear analysis. Therefore, for the determination of the buckling load of the imperfect structure, all four models listed in Table 1 may be expected to be appropriate.

Table 1
Numerical models for shells of revolution with eigenmode-affine imperfections

Model type	Model details	Obvious reasons for adoption in nonlinear analysis	Advantages or disadvantages in bifurcation analysis
Whole structure	The complete structure is modelled.	Availability of a powerful computer and convenience for plotting	Bifurcation loads can be determined without revisions to the numerical model.
Half structure	Half of the structure obtained by cutting the structure vertically across a diametrical plane is included with symmetry conditions imposed along the meridional edges.	As good as a complete model for structures whose deformations are at least symmetric about one vertical diametrical plane but computationally more efficient	Bifurcation loads can be determined without revisions to the numerical model.
Whole wave	A sector model spanning over one complete circumferential wave is used, with symmetry conditions imposed along the meridional edges.	Computationally efficient; more convenient for graphical examination of deformations compared to the half-wave sector model.	Many revisions to the numerical model are needed in the search for the lowest buckling load.
Half wave	A sector model spanning over half a circumferential wave is used, with symmetry conditions imposed along the meridional edges.	Computationally most efficient	Many revisions to the numerical model are needed in the search for the lowest buckling load.

Example studies which used half-structure, whole-wave and half-wave models include Guggenberger (1995, 1996), Knebel and Schweizerhof (1995), Goto and Zhang (1999) and Pircher et al. (1999). The choice of a particular model depends on its suitability for both the nonlinear analysis of the imperfect structure and the linear or nonlinear bifurcation analysis of the perfect structure, since the latter needs to be carried out before the former to determine the eigenmode. Therefore, Table 1 gives the obvious reasons for adopting the various models in the nonlinear analysis of the imperfect structure, together with the advantages or disadvantages of the models in a bifurcation analysis of the perfect structure. In addition, plotting requirements and available computing power also influence the choice of a particular numerical model.

In practical applications, a mixture of different models may be used to advantage for any given problem. For example, a nonlinear bifurcation analysis can be carried out using the half-structure model, which is then followed by a nonlinear analysis of the imperfect shell using the half-wave model. Such combinations are a further factor of influence in the choice of numerical models.

3. Performance of different numerical models

A cylinder subject to a radial ring load q (Fig. 1) was used to compare the performances of three of the four numerical models: half-structure, whole-wave and half-wave models. The whole-structure model was excluded from the comparison as the half-structure model was expected to show the same behaviour characteristics. The whole-structure model is considered in the comparison of buckling loads later. The two ends of the cylinder were restrained from radial and circumferential displacements only. As the structure possesses symmetry about the mid-height plane, the problem was simplified down to a cylinder half the length of the original one, with one end restrained against axial displacements and meridional rotations, and the other end restrained against radial and circumferential displacements. For clarity of terminology, it is better simply to refer to this cut cylinder as the original structure, while the half-structure model refers to this cut cylinder, cut again vertically. Deformation modes antisymmetric about the mid-height were not found to be critical for the ring loaded cylinder and the use of the cut cylinder structure precluded any such modes. This restriction does not detract from the generality of the conclusions reached here even if such antisymmetric modes should have been critical had the entire cylinder been modelled.

A thorough study of this problem, as a simple typical problem of a cylinder under local circumferential compression is given in Song and Teng (2000), where the accuracy of the ABAQUS models is also demonstrated through comparisons of bifurcation buckling loads from ABAQUS and the well-tested NEPAS program for shells of revolution (Teng and Rotter, 1989). As mentioned earlier, all results presented in this paper were obtained using ABAQUS. The cylinder examined here has a thickness $t = 1$ mm, a radius-to-thickness ratio $R/t = 500$ and a length-to-radius ratio $L/R = 3$. The elastic modulus $E = 2 \times 10^5$ MPa and Poisson's ratio $v = 0.3$. This cylinder was predicted by ABAQUS to have a linear bifurcation load q_{cr}^{L} of 7.566 N/mm with eight circumferential buckling waves (i.e. $n_{cr} = 8$) and a nonlinear bifurcation load q_{cr}^{N} of 6.920 N/mm with 15 circumferential buckling waves. The nonlinear bifurcation analysis took into account the effect of prebuckling deformations which led to a small reduction in the buckling load but a large increase in the number of buckling waves. The linear and nonlinear bifurcation modes are shown in Fig. 2. In the present study, the imperfections were assumed to be in the form of the nonlinear bifurcation mode.

The half-wave model is the simplest of the three models being considered. The load–deflection curves obtained using the arc-length method (Wempner, 1971; Riks, 1979; Crisfield, 1981; Ramm, 1981) as implemented in ABAQUS for half-wave models of a ring-loaded cylinder with eigenmode-affine geometric imperfections of different amplitudes are shown in Fig. 3. The vertical axis in Figs. 3–5, 7, 9, 10 and 12 is the load factor over the nonlinear bifurcation load, so a value of 0.8, e.g., for the maximum load factor indicates a 20% reduction in the buckling load due to an imperfection. The horizontal axis in the same figures

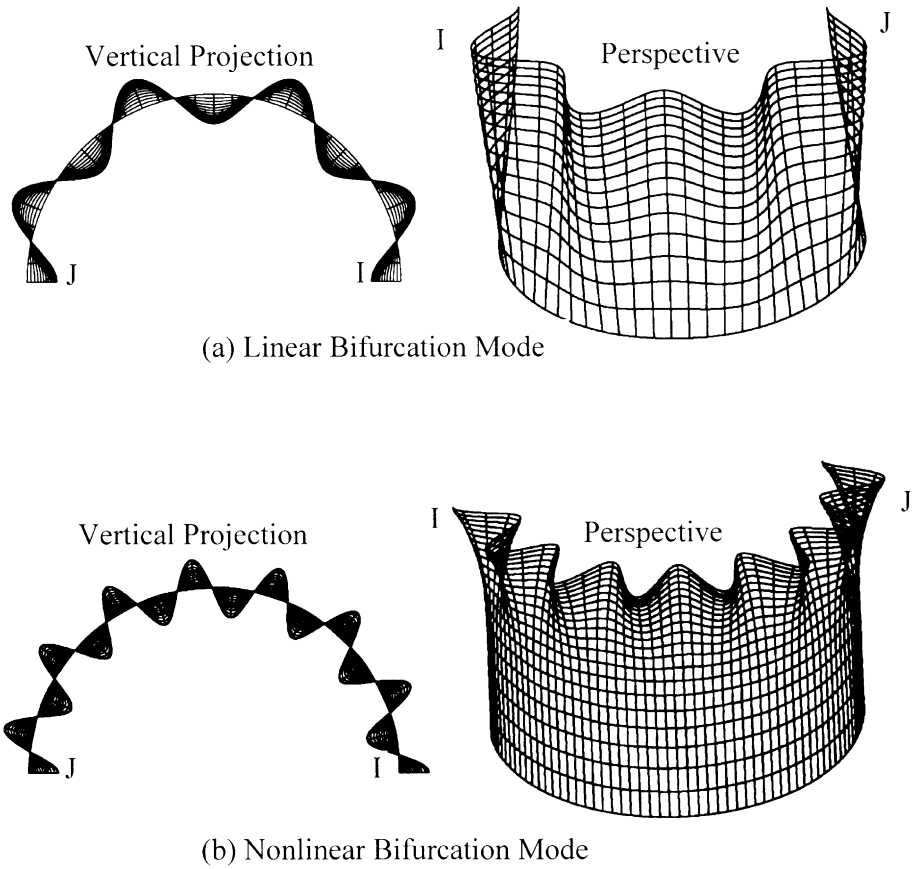

Fig. 2. Linear and nonlinear bifurcation modes: (a) linear bifurcation buckling mode and (b) nonlinear bifurcation mode.

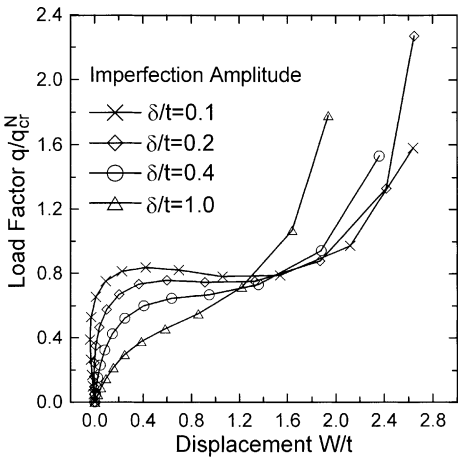

Fig. 3. Load–deflection curves from half-wave sector models.

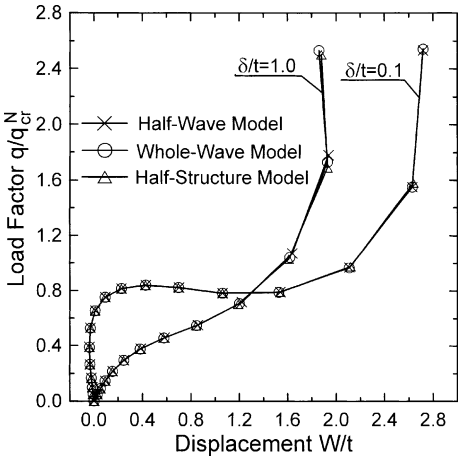

Fig. 4. Comparison of load–deflection curves between three different models.

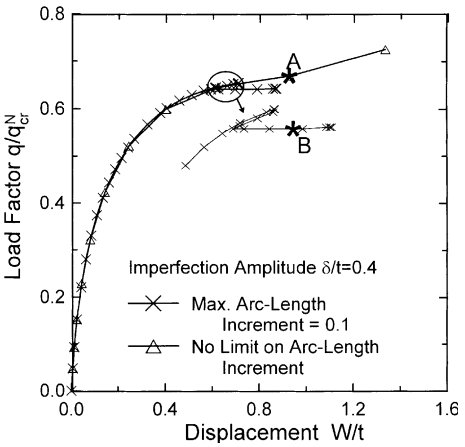

Fig. 5. Effect of an arc-length increment limit on the load–deflection curve of a half-structure model.

is the radial displacement normalized by the shell thickness at the wave crest in both the half-wave model and the whole-wave model, or that of point I in the half-structure model (Fig. 2).

Fig. 3 shows that the shell is rather sensitive to geometric imperfections, but a limit point cannot be found on the load–deflection curve when a reasonably large imperfection is present. Fig. 4 compares the results from the three numerical models. They are identical as expected.

The curves shown in Figs. 3 and 4 are not so smooth as only a small number of converged points were available. When the calculations were repeated to obtain better curves by limiting the maximum increment in the normalized arc-length as used in ABAQUS, surprising results were obtained. The results are shown in Fig. 5 for an imperfection amplitude $\delta/t = 0.4$. The results from the whole-wave and half-wave models with the maximum increment in arc-length $\Delta l_{\max}$ limited to 0.1 are similar to those without such a limit (not shown here). However, the results from the half-structure model are surprisingly affected by this limit (Fig. 5). In particular, the new load–deflection curve has a limit point at a load of 0.654 $q_{\mathrm{cr}}^{\mathrm{N}}$ N/mm. The deformed shapes of the half-structure model for two points (points A and B) on the two load–deflection curves of Fig.

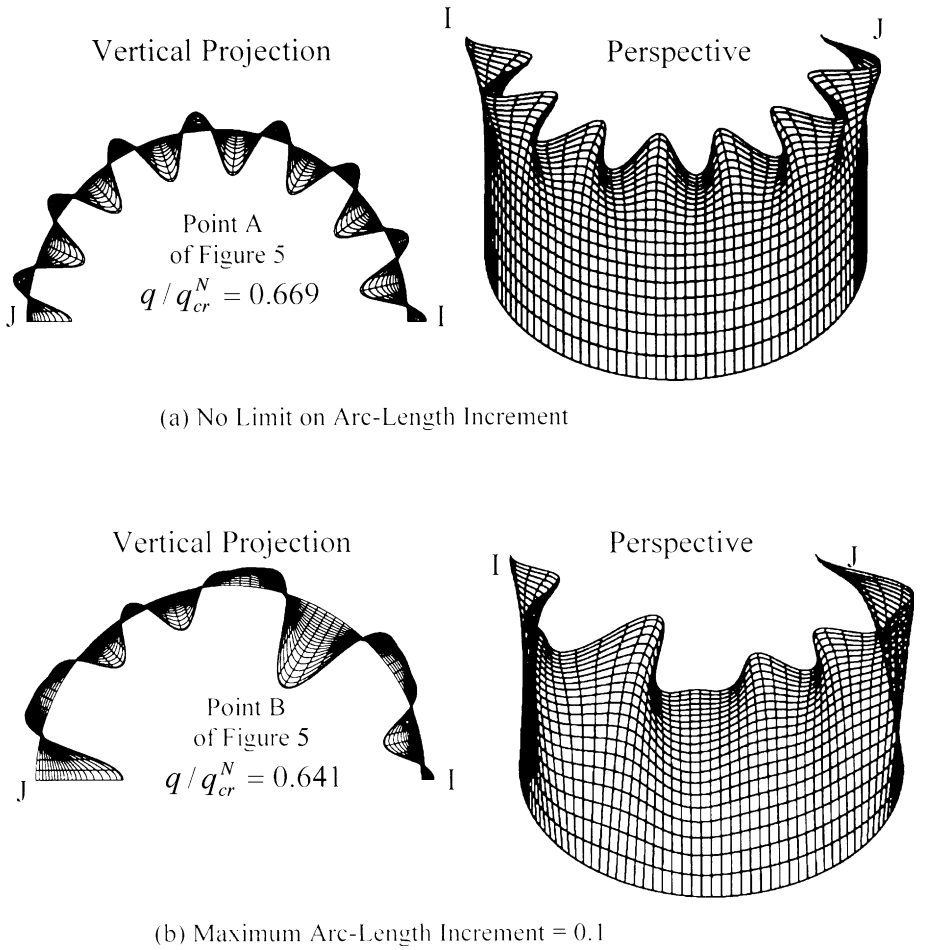

Fig. 6. Deformed shapes of a half-structure model: (a) maximum arc-length increment not limited and (b) maximum arc-length increment = 0.1.

5 are illustrated in Fig. 6. The deformed shape of the shell obtained without a limit on the arc-length increment has the same number of periodical waves as the imperfection, while that with a limit on the arc-length increment has large localized deformations in two zones. Furthermore, it was found that using the half-structure model, the limit point load also changed with the finite-element mesh when a limit was imposed on the arc-length increment (Fig. 7). The meshes considered here had 12 nodes, 16 nodes, 24 nodes and 32 nodes per circumferential wave of the imperfection with the vertical divisions being the same. The dimensionless limit point loads $q/q_{\mathrm{cr}}^{\mathrm{N}}$ for the four different meshes are 0.649, 0.654, 0.804 and 1.530. The different meshes all resulted in the same load–deflection response in the initial stage, so the meshes were all fine enough to model the deformations of the structure accurately. This situation contrasts with that for the whole-wave and half-wave models for which the load–deflection curves were not found to depend on the finite-element mesh.

While an arc-length increment limit of 0.1 was used in obtaining the results presented in Figs. 5 and 7, it should be noted that the particular value of this limit should not be given too much significance. The important observation is that if the arc-length increment is limited to be sufficiently small, then the predicted

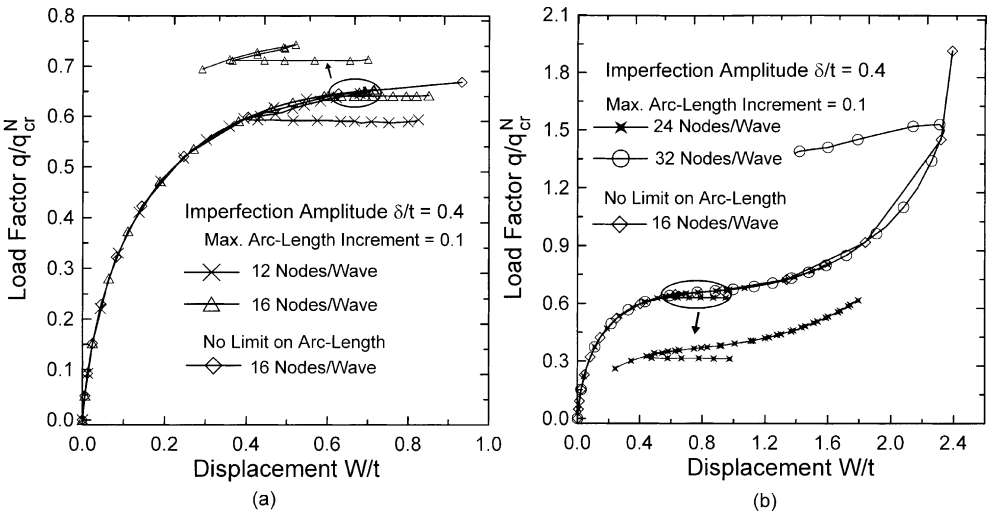

Fig. 7. Mesh dependence of the load–deflection curves.

response will be affected by such a limit. For the cases considered in Figs. 5 and 7, while a limit of 0.05 was found also to affect the predicted response, a limit of 0.5 was found to have no appreciable effect on the prediction.

Based on the above discussions, one might be inclined to conclude that both the whole-wave and half-wave models may be used in nonlinear analysis, while the half-structure model is unreliable. The validity of this conclusion is challenged in Section 4.

4. Nonlinear bifurcation of imperfect shells

The dependence of the limit point buckling load of a shell with a significant eigenmode-affine imperfection on mesh refinements and solution procedures was initially surprising. Subsequently, it was realized that the sensitivity of the behaviour to details in the solution method arose from the existence of a bifurcation point along the primary path of the imperfect shell. The primary path of the imperfect shell refers to its deformation path with the deformation mode being that imposed by the eigenmode-affine imperfection. As the shell advances along the primary path, the eigenmode-affine imperfection is amplified and modified in shape. The total deformations are the sum of an axisymmetric component and a non-axisymmetric component that is initially in the form of a single harmonic but gradually evolves into one accurately describable only by the sum of a number of harmonic terms.

A careful check of the ABAQUS output did identify some signs of a bifurcation point: the program reported for both the whole-wave and half-structure models that there was a negative eigenvalue at a certain load level, which meant that a bifurcation point had been passed for these models. For the half-wave model, such a bifurcation point was not indicated and was nonexistent due to the imposed symmetry conditions along two closely-spaced meridional generators.

To find the precise buckling load of the imperfect shell, the exact location of the bifurcation point on the primary deformation path is required. Provided this bifurcation point leads to a descending path, then the bifurcation load represents the ultimate strength of the imperfect shell. A nonlinear bifurcation analysis for the half-structure model of the imperfect shell with an imperfection amplitude $\delta/t = 0.4$ gave a bifurcation load of 0.651 q_{cr}^{N}. The corresponding nonlinear bifurcation mode is shown in Fig. 8.

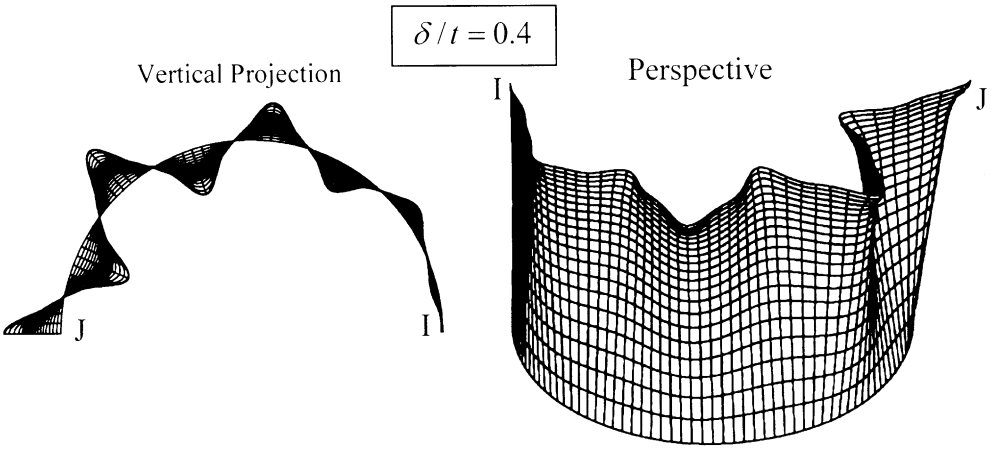

Fig. 8. Nonlinear bifurcation mode of an imperfect cylinder.

The effect of a limit on the maximum arc-length increment discussed in Section 3 can now be explained as follows. Ideally, the shell should deform along the primary path, if no disturbance exists to induce the shell to deform along the post-bifurcation path. This is the case for the analyses carried out without a limit on the maximum arc-length increment (Figs. 3 and 4). In such analyses, disturbances from numerical round-off errors were too small to cause the shell to deform along a post-bifurcation path. With the imposition of a limit on the arc-length increment, more loading steps and iterations were required in the analysis process, leading to greater numerical round-off errors. With this limit being sufficiently small, these numerical errors were then significant enough to induce the shell to deform along a post-bifurcation path. It should be noted that there is no guarantee at all that these numerical errors will turn the shell deformation path at the correct bifurcation load or to lead it along the correct post-bifurcation path (Fig. 7). In two of the cases considered in Fig. 7, the peak load is close to the actual bifurcation load (Fig. 7a), while in the other two cases the peak load is significantly higher than the actual bifurcation load. For the latter two cases, the analysis was found to fall back on the original load–deflection curve in one case and to go on to a higher post-bifurcation path in the other (Fig. 7b). Therefore, even when random numerical round-off errors do induce the shell to follow a post-bifurcation path, the limit point load so predicted cannot be relied on as the correct bifurcation load or a close approximation of it.

5. Post-bifurcation analysis of imperfect shells

To find out if a bifurcation point leads to a descending load-deflection path, nonlinear analyses are required in which the imperfection included a small component in the form of the nonlinear bifurcation mode of the imperfect shell. Such analyses were carried out for three different imperfection amplitudes in the present investigation. An imperfection of the following form was used:

$$\{U_t\} = \frac{\delta}{t}[\{U_0\} + 0.01\rho\{U_a\}],$$

where $\{U_0\}$ is the normalized nonlinear bifurcation mode of the perfect shell and $\{U_a\}$ is the normalized nonlinear bifurcation mode of the imperfect shell. Both bifurcation modes are bi-directional in nature, i.e., the maximum bifurcation displacement can be inwards or outwards. For simplicity of description here, the directions of the two bifurcation modes are assumed to be positive when the combined imperfection with

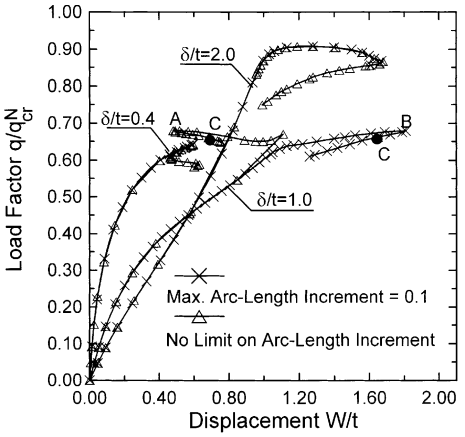

Fig. 9. Independence of limit point loads of the arc-length increment.

$\rho = 1$ (i.e. when they are added together) has an amplitude greater than that of the original eigenmode-affine imperfection.

Three cases were considered: $\delta/t = 0.4$, 1 and 2. Fig. 9 shows the load–deflection curves for these three cases with or without a limit for the arc-length increment with $\rho = 1$. It is first appropriate to examine the case of $\delta/t = 1$, where an arc-length increment limit is found to change the path. Furthermore, the initial peak at $q/q_{cr}^{N} = 0.670$ of the load–deflection curve obtained with no limit on the arc-length increment disappears in the curve obtained with a limit of 0.1 for the arc-length increment. The second peak (point A) of the former curve at $q/q_{cr}^{N} = 0.680$ corresponds to the peak at $q/q_{cr}^{N} = 0.679$ (point B) on the latter curve. All three peak loads are a little higher than the dimensionless nonlinear bifurcation load of the imperfect shell which is 0.646. This difference in behaviour is surprising but can be explained if Fig. 10 is examined carefully.

In Fig. 10, the primary path of the imperfect shell with an eigenmode-affine imperfection only is shown together with two post-bifurcation paths which emanate from the primary path for each of the three values of δ/t. These two post-bifurcation paths correspond to two different choices of the direction of the second component of imperfection ($\rho = 1$ and $\rho = -1$). This indicates that the two paths followed in Fig. 9 in fact correspond to two different post-bifurcation paths, due to influences from small random numerical round-off errors. Fig. 10b shows that the initial peaks on the load–deflection curves obtained when the arc-length increment was not limited disappear once a limit was imposed. The rounding of these initial peaks can be attributed to the greater numerical errors due to the imposition of a limit on the arc-length increment. Further, it is interesting to note that a limit on the arc-length increment also reversed the directions of the post-bifurcation paths followed by the analyses (Fig. 10b).

The deformed shapes for the shell with $\delta/t = 1$ correspond to points C on the two load–deflection curves of the two different conditions of arc-length increments (Fig. 9) differ basically by a circumferential shift, while the overall patterns of the deformations for the two cases are very similar (Fig. 11). For the other cases, ($\delta/t = 0.4$ and $\delta/t = 2$), such a shift in deformation pattern was not induced by numerical round-off errors.

Table 2 lists the limit point loads and the nonlinear bifurcation loads for all three imperfect cylinders with $\rho = 1$. For $\delta/t = 0.4$ and 2, the bifurcation loads of the imperfect shells are very close but slightly higher than the corresponding limit point loads, indicating that the bifurcation load is the upper limit of the ultimate strength of the imperfect shell for these cases. For the other shell with $\delta/t = 1$, the limit point loads are slightly higher than the corresponding bifurcation loads. For the two load–deflection curves obtained

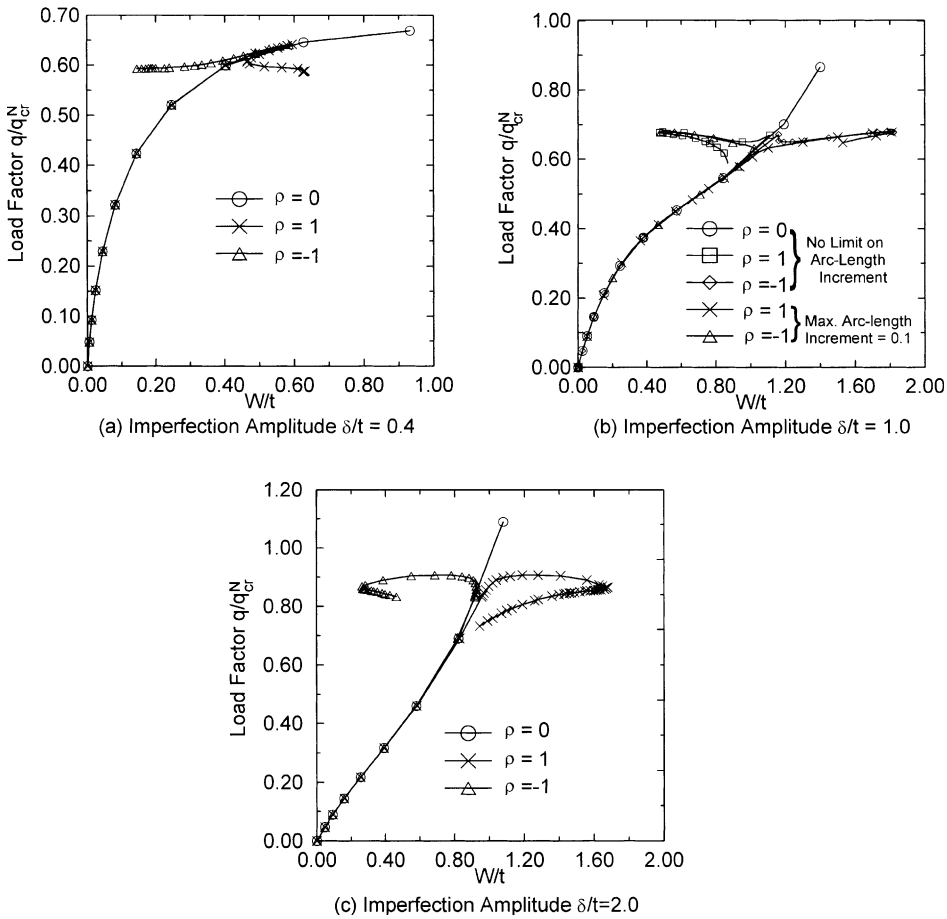

Fig. 10. Load–deflection curves of three imperfect cylinders.

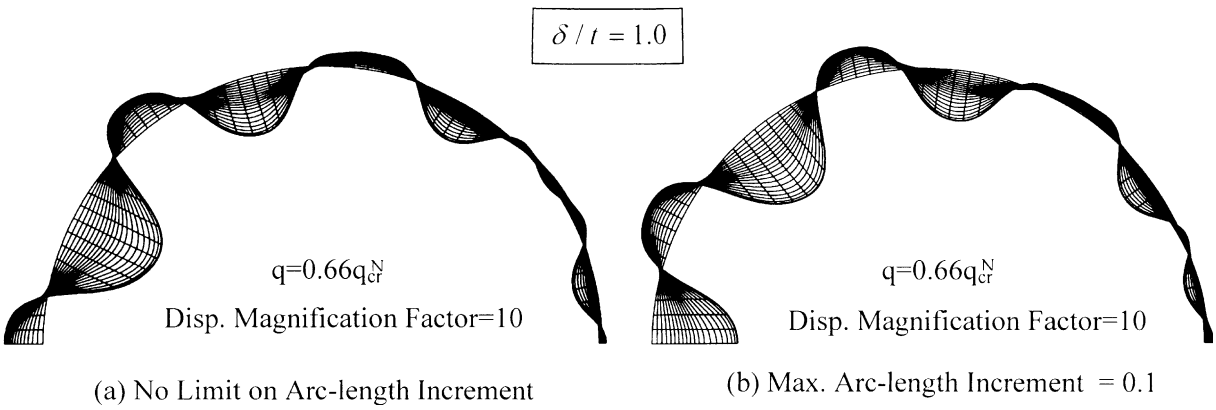

Fig. 11. Circumferential shift of deformations as a result of limiting the arc-length increment.

Table 2
Comparison of nonlinear bifurcation loads and limit point loads

δ/t	Nonlinear bifurcation load q/q_{cr}^{N}	Limit point load $q/q_{cr}^{N}(\rho = 1)$	
		No limit on arc-length increment	Arc-length increment limited to 0.1
0.4	0.651	0.641	0.642
1	0.646	0.680	0.670
2	0.909	0.908	0.908

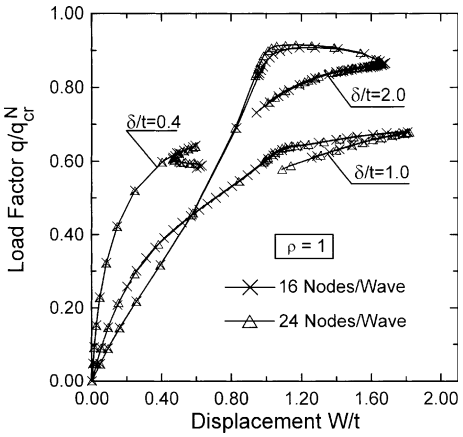

Fig. 12. Independence of limit point loads of mesh refinements.

with a limit for the arc-length increment, the higher limit loads are attributable to a weakly stable initial post-bifurcation path (Fig. 10b). For the other two curves, the reason for the initial peak loads being higher than the bifurcation load is not so easy to pinpoint given the complex processes involved in the analyses. These results demonstrate the complexity involved in nonlinear analyses to determine the buckling strength of shells. Despite this complication, the limit point loads of these shells with complex imperfections are basically independent of the arc-length increment (Table 2).

Fig. 12 demonstrates the insensitivity of the limit point load to mesh refinements, although a small difference is seen between the two meshes explored for the case of $\delta/t = 2$ (less than 1% difference for the limit point load).

6. Comparison of buckling loads of imperfect shells

Since the buckling load of the imperfect shell was of primary interest, this buckling load was determined for imperfections of various amplitudes using the four different numerical models and given in Table 3. For all models, the buckling load is the limit point load when $\delta/t = 0.1$ and 0.2 as no bifurcation point exists before the limit point. For other values of δ/t, the buckling load is taken to be that of the inflection point (Yamaki, 1984) of the load–deflection curve for half-wave models (underlined values in Table 3), and the nonlinear bifurcation load of the imperfect shell for other models. The latter treatment represents a relatively simple and close approximation for the present problem, as the post-bifurcation path of the imperfect shell may be weakly stable and thus may lead to a limit point slightly higher than its nonlinear bifurcation load (Fig. 10).

Table 3
Comparison of buckling loads

δ/t	0.1	0.2	0.4	0.6	0.8	1.0	1.2	1.6	2.0
Half wave	0.838	0.758	0.659	0.603	0.551	0.510	0.468	0.406	0.320
Whole wave	0.838	0.758	0.650	0.587	0.588	0.637	0.691	0.800	0.905
Half structure	0.838	0.758	0.651	0.593	0.596	0.646	0.701	0.809	0.909
Whole structure	0.838	0.758	0.650	0.593	0.595	0.647	0.704	0.817	0.916
(spurious mode)					(0.578)	(0.539)	(0.505)	(0.453)	(0.418)

The differences between the buckling loads of the half-wave model and the other models are large. One may dismiss the validity of the inflection point method as being appropriate for the determination of the buckling load, but if this method is dismissed, no other suitable methods seem apparent. Apart from the buckling loads, there are important differences between the post-buckling responses predicted by the half-wave model and the other models. The half-wave model precluded any bifurcation due to the imposition of symmetry conditions along the two meridional edges. The stable post-buckling curve means that the ultimate strength of the shell can only be limited by material yielding. As the half-wave model leads to incorrect buckling loads and post-buckling responses, it is not suitable for the present problem.

On the other hand, the whole-wave model is seen to predict the buckling loads closely for this problem. The advantage of the whole-wave model is its computational efficiency, but whether this model can always predict the buckling load closely is uncertain. A whole-wave model allows some possibilities of bifurcation of the imperfect shell. If the bifurcation mode corresponds to a load near the lowest bifurcation load of the whole-structure model, the whole-wave model leads to a close prediction of the buckling load. Similarly, whether the whole-wave model predicts a post-buckling path close to the actual post-buckling path is also uncertain.

The half-structure model has many advantages over the other models. It predicts accurately the buckling load and mode, and is computationally much more efficient than the whole-structure model. The whole-structure model is expected to give the most reliable answer as it is given no artificial constraint. In most cases, however, a vertical plane of symmetry exists in the deformations, and the half-structure model is as good as the whole-structure model.

The whole-structure model was found to have another disadvantage in addition to being computationally most inefficient; it is more likely to experience spurious modes such as that shown in Fig. 13 for $\delta/t = 1$. These spurious modes are likely to be suppressed by imposed symmetry conditions along the two meridional edges in the half-structure model. The whole issue of spurious modes in nonlinear bifurcation analysis is very complicated, and will not be dealt with in detail here. For the present purpose, it is important to note that a negative eigenvalue, while indicating a bifurcation of deformation path in most cases, can correspond to a spurious mode. For the ring loaded cylinder considered here, the first bifurcation mode found was often a spurious mode. The bifurcation loads correspond to the spurious modes are also listed in Table 3. This shows that in order to determine the buckling strength of a shell with eigenmode imperfections, it is not sufficient just to locate the bifurcation point; the bifurcation mode should be inspected to ensure that the mode is realistic. Fig. 14 shows the correct nonlinear bifurcation mode of an imperfect shell with $\delta/t = 0.4$. This mode is found to match well with that obtained using the half-structure model (Fig. 8).

It should be remarked that in all cases where nonlinear bifurcation rather than limit point buckling is the critical, the buckling loads predicted by the half-structure model are slightly higher than those by the whole-wave model. For the larger imperfection amplitudes considered, the buckling loads of the whole-structure model are slightly higher than those of the half-structure model, although in most cases the whole-structure and half-structure models agree with each other closely. The above phenomenon is contrary to conventional beliefs, but these differences are very small.

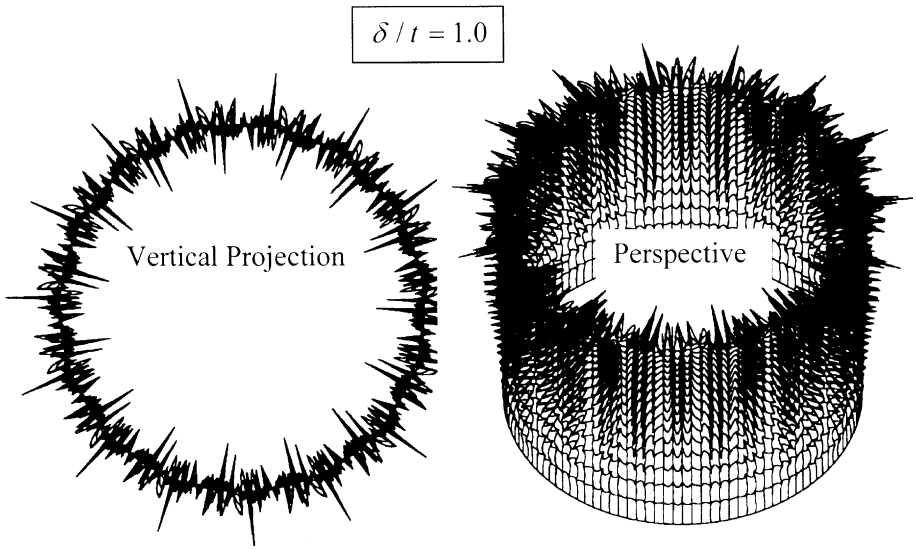

Fig. 13. Spurious bifurcation mode of a whole-structure model for an imperfect cylinder.

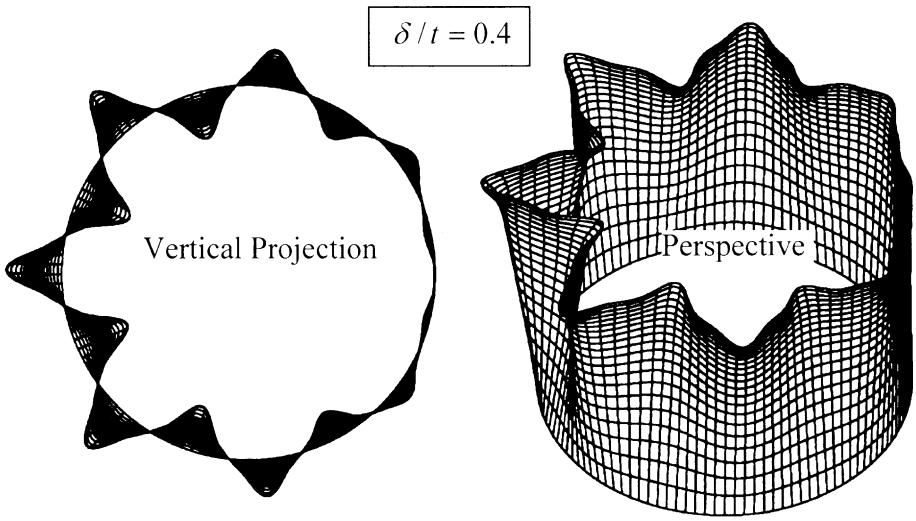

Fig. 14. Nonlinear bifurcation mode of a whole-structure model for an imperfect cylinder.

7. Cases requiring a whole-structure model

The preceding discussions may lead to the assertion that the half-structure model should be able to capture all deformation modes and is as good as the whole-structure model for axisymmetrically loaded shells of revolution with eigenmode-affine imperfections. Is there then a need at all for the whole-structure model for such problems? The externally pressurized cylinder provides an interesting example for which the whole-structure model is required.

Post-buckling behaviour of cylinders under external hydrostatic pressure has been investigated both experimentally and numerically (Esslinger and Geier, 1975; Yamaki, 1984; Guggenberger, 1996). A striking feature of the post-buckling response is that the observed final failure is in a torsional mode. This was first observed by Esslinger and Geier (1975) and recently further studied by Guggenberger (1996).

Guggenberger (1996) appears to be the first to have reproduced the torsional failure mode with the finite-element method. A whole-wave model was used in his analysis in which 'cyclic' boundary conditions were used for the two meridional edges instead of the conventional symmetry boundary conditions so that torsional deformations were possible. A small torsional disturbance force was applied to trigger the shell to deform into the torsional failure mode and then subsequently removed. This approach is not realistic if the physical phenomenon is not known a priori, so it cannot be generally applicable. As pointed out by Guggenberger, if symmetric boundary conditions are used for the meridional edges in a whole-wave model, no torsional deformations will occur. On the other hand, such torsional deformations can be easily accommodated by a whole-structure model, although the model may still be unable to predict the torsional mode without any intervention.

The shell considered here has the same geometric and material properties as those assumed by Guggenberger (1996): length $L = 400$ mm, radius $R = 200$ mm, thickness $t = 1$ mm, elastic modulus $E = 3200$ MPa, and Poisson's ratio $v = 0.35$. The bottom end was completely clamped, while the top end was closed by a rigid circular steel plate.

Fig. 15 shows two load–deflection curves of the shell with an imperfection in the shape of the first linear buckling mode of the perfect shell ($n_{cr} = 8$). The imperfection amplitude $\delta/t = 2$. The only difference between these two curves is the choice of the maximum arc-length increment. The analysis with a smaller arc-length increment limit produced curve II which indicates a mode change at point A ($q/q_{cr}^{L} = 1.28$), but the one with a larger limit could not predict this mode change. Point A was confirmed by a nonlinear bifurcation analysis of the imperfect shell to be a true bifurcation point. Fig. 16 shows the nonlinear bifurcation mode of the imperfect shell, where torsional deformations are evident.

Fig. 17 shows typical deformed shapes of the three phases of curve II: OA, AB, and BC, where the change of deformation mode is clearly seen. The deformed shapes correspond to positions indicated by large circles on the load–deflection curve. The automatic transition of the deformation path predicted by the analysis with a smaller arc-length limit is attributable to accumulated numerical round-off errors. With a smaller value for the maximum arc-length increment, more loading increments and equilibrium iterations were needed, which in turn led to larger numerical round-off errors.

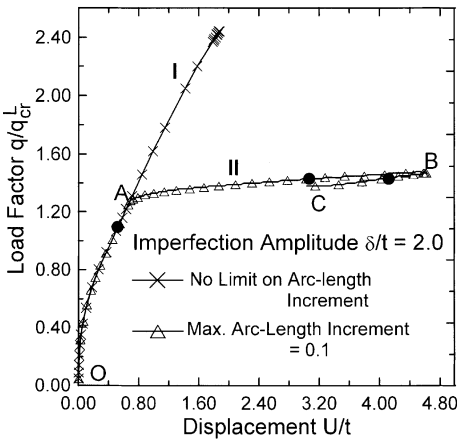

Fig. 15. Load–deflection curves of an externally pressurized cylinder.

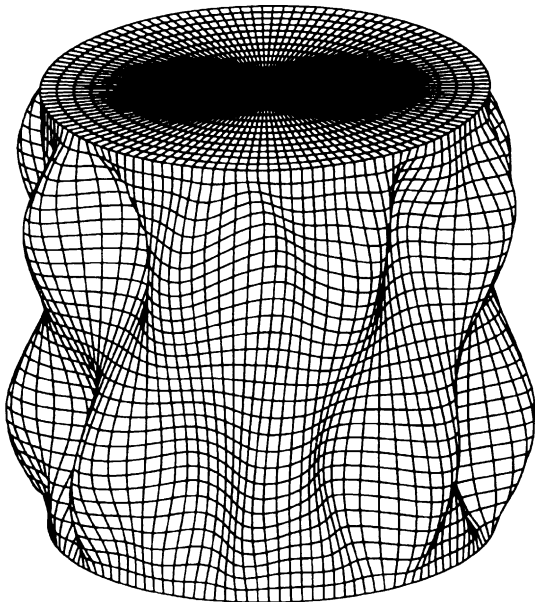

Fig. 16. Nonlinear bifurcation mode of an externally pressurized imperfect cylinder.

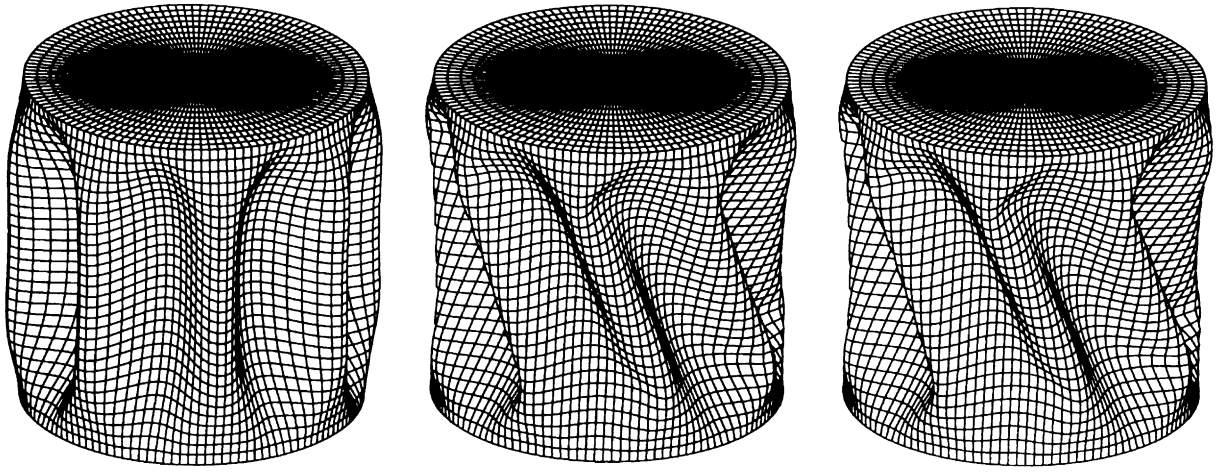

Fig. 17. Mode changes in an externally pressurized cylinder.

The same problem was analysed using a half-structure model, which predicted a maximum load-carrying capacity of $q = 2.37q_{cr}^{L}$ with the maximum arc-length increment limited to 0.1. This shows that even for the prediction of the maximum load carrying capacity, the inclusion of the whole structure model is necessary

in some cases. This is the case if the maximum load coincides with a deformation mode change that destroys the symmetry conditions imposed on the two meridional edges lying at the ends of a diametrical plane in the half-structure model. The torsional deformations of the shell was also not correctly predicted by the half-structure model.

8. Conclusions

This paper has discussed a number of issues needing particular care by numerical analysts in predicting the buckling strength of axisymmetrically loaded elastic shells of revolution with eigenmode-affine imperfections using a general curved thin shell element. It is likely that there are other pitfalls in the nonlinear analysis of shells, so there is no place for complacence for such analyses. Within the limitation of elastic behaviour, the following conclusions can be drawn from this study:

(1) The simplistic belief, which is correct for systems with simple buckling behaviour, that an eigenmode imperfection converts the bifurcation buckling problem to a limit point problem and hence the load carrying capacity can be determined by a straightforward nonlinear analysis can lead to erroneous results. This is because a shell may experience mode changes in the deformation process before reaching the limit point. While mode changes have generally been associated with post-buckling behaviour of perfect shells, the present study shows that mode changes are also important in prebuckling deformations of imperfect shells.

(2) An axisymmetrically-loaded shell of revolution with an eigenmode-affine imperfection possesses periodical symmetry which has often been exploited in building numerical models. The existence of one or more bifurcation points along the deformation path means that such symmetry is not maintained throughout the process of deformation, so its exploitation in analysis may lead to erroneous results.

(3) A nonlinear bifurcation analysis of the deformed imperfect shell without the imposition of incompatible symmetry conditions is necessary to guarantee the correct prediction of any bifurcation point and the buckling strength. While random numerical round-off errors may induce the shell to deform along a post-bifurcation path, the bifurcation load and the post-bifurcation path so obtained are not reliable and are sensitive to mesh refinements and details of the solution procedure.

(4) A whole-structure model with bifurcation behaviour continuously monitored and followed should be capable of predicting the correct buckling load, provided that spurious bifurcation modes are weeded out in the analysis by checking the nonlinear bifurcation modes or guarded against by the use of more sophisticated shell elements.

(5) A half-structure model should be as good as a whole-structure model provided a vertical diametrical plane of symmetry exists for the deformations and does not seem to suffer from the spurious mode problem.

(6) If the buckling load is the main parameter of interest and it can be ascertained that no bifurcation point exists before reaching the limit point buckling load even when the whole-structure is modelled, the half-wave model is then an accurate and very efficient model. The predicted load–deflection path is that of a shell deforming in a periodical mode imposed by the eigenmode-affine imperfection.

(7) The whole-wave model allows some possibilities of bifurcation. For the present problem, it predicts the buckling load well, although the deformation mode cannot be correctly predicted. If it can be shown that the whole-wave model is generally capable of delivering the buckling load accurately, though with some errors in the deformed shape, it can be a useful model for practical applications as it is very economic. Further research should be carried out on the wider suitability of the whole-wave model.

Finally, it should be noted that, in the presence of material plasticity, some of the observations made will have to be modified. A similar study on shells with elastic–plastic material behaviour should be carried out in the future.

Acknowledgements

Both authors are grateful to the Research Grants Council of the Hong Kong Special Administrative Region (Project No. PolyU 5081/97E) and The Hong Kong Polytechnic University for their financial support.

References

Arbocz, J., 1997. Future directions and challenges in shell stability analysis. Proceedings of 38th AIAA/ASME/ASCE/AHS/ASC Structures, Structural Dynamics and Material Conference, Part 3 (of 4), 1949–1962.

Chryssanthopoulos, M.K., Baker, M.J., Dowling, P.J., 1991a. Statistical analysis of imperfections in stiffened cylinders. ASCE Journal of Structural Engineering 117 (7), 1979–1997.

Chryssanthopoulos, M.K., Baker, M.J., Dowling, P.J., 1991b. Imperfection modeling for buckling analysis of stiffened cylinders. ASCE Journal of Structural Engineering 117 (7), 1998–2017.

Crisfield, M.A., 1981. A fast incremental/iterative solution procedure that handles 'snap-through'. Computer and Structures 13, 55–62.

ENV 1993-1-6 (1999) Eurocode 3: Design of Steel Structures, Part 1.6: General Rules-Supplementary Rules for the Strength and Stability of Shell Structures, Draft Standard, CEN, Brussels.

Esslinger, M., Geier, B., 1975. Postbuckling Behavior of Structures. Springer, Berlin.

Goto, Y., Zhang, C., 1999. Plastic buckling transition modes in moderately thick cylindrical shells. ASCE Journal of Engineering Mechanics 125 (4), 426–434.

Guggenberger, W., 1995. Buckling and postbuckling of imperfect cylindrical shells under external pressure. Thin-Walled Structures 23, 351–366.

Guggenberger, W., 1996. Analysis of the torsional postbuckling mode of externally pressurized circular cylindrical shells. European Workshop on Thin-Walled Steel Structures. Krzyzowa, Poland.

Hibbit, Karlsson & Sorensen, 1998. ABAQUS Version 5.8. Standard User's Manual.

Knebel, K., Schweizerhof, K., 1995. Buckling of cylindrical shells containing granular solids. Thin-Walled Structures 23, 295–312.

Pircher, M., O'Shea, M., Bridge, R., 1999. The influence of weld-induced residual stresses on the buckling of cylindrical thin-walled shells. In: Shanmugam, N.E., Richard Liew, J.Y., Thevendran, V. (Eds.), Thin-Walled Structures Research and Development. Elsevier, London, pp. 671–678.

Ramm, E., 1981. Strategies for tracing nonlinear response near limit points. In: Wunderlich, W., Stein, E., Bathe, K.J. (Eds.), Nonlinear Finite Element Analysis in Structural Mechanics, Springer, New York, pp. 63–89.

Riks, E., 1979. An incremental approach to the solution of snapping and buckling problems. International Journal of Solids and Structures 15, 529–551.

Rotter, J.M., 1998. Shell structures: the new european standard and current research needs. Thin-Walled Structures 31 (1–3), 3–23.

Schmidt, H., Krysik, R., 1991. Towards recommendations for shell stability design by means of numerically determined buckling loads. In: Jullien, J.-F. (Ed.), Proceedings of International Colloquium on Buckling of Shell Structures, on Land, in the Sea and in the Air. Lyon, France, pp. 508–519.

Speicher, G., Saal, H., 1991. Numerical calculation of limit loads for shells of revolution with particular regard to the applying equivalent initial imperfections. Proceedings of International Colloquium on Buckling of Shell Structures, on Land, in the Sea and in the Air. Lyon, France, pp. 466–475.

Song, C.Y., Teng, J.G., 2000. Buckling and postbuckling of cylinders under a radial ring load, in preparation.

Teng, J.G., 1996. Buckling of thin shells: recent advances and trends, applied mechanics reviews. ASME 49 (4), 263–274.

Teng, J.G., Rotter, J.M., 1989. Non-symmetric bifurcation of geometrically non-linear elastic–plastic axisymmetric shells subject to combined loads including torsion. Computers and Structures 32 (2), 453–477.

Wempner, G.A., 1971. Discrete approximations related to nonlinear theories of solids. International Journal of Solids and Structures 7, 1581–1599.

Yamaki, N., 1984. Elastic Stability of Circular Cylindrical Shells. North-Holland, Amsterdam.